



## Characterization of Primary Cilia in Human Airway Smooth Muscle Cells

Jun Wu, MD; Hui Du, PhD; Xiangling Wang, PhD; Changlin Mei, MD; Gary C. Sieck, PhD; and Qi Qian, MD

**Background:** Considerable evidence indicates a key role for primary cilia of mammalian cells in mechanochemical sensing. Dysfunctions of primary cilia have been linked to the pathogenesis of several human diseases. However, cilia-related research has been limited to a few cell and tissue types; to our knowledge, no literature exists on primary cilia in airway smooth muscle (ASM). The aim of this study was to characterize primary cilia in human ASM.

**Methods:** Primary cilia of human bronchial smooth muscle cells (HBSMCs) were examined using immunofluorescence confocal microscopy, and scanning and transmission electron microscopy. HBSMC migration and injury repair were examined by scratch-wound and epidermal growth factor (EGF)-induced migration assays.

**Results:** Cross-sectional images of normal human bronchi revealed that primary cilia of HBSMCs within each ASM bundle aggregated at the same horizontal level, forming a “cilium layer.” Individual cilia of HBSMCs projected into extracellular matrix and exhibited varying degrees of deflection. Mechanochemical sensing molecules, polycystins, and  $\alpha 2$ -,  $\alpha 5$ -, and  $\beta 1$ -integrins were enriched in cilia, as was EGF receptor, known to activate jointly with integrins during cell migration. Migration assays demonstrated a ciliary contribution to HBSMC migration and wound repair.

**Conclusions:** The primary cilia of ASM cells exert a role in sensing and transducing extracellular mechanochemical signals and in ASM injury repair. Defects in ASM ciliary function could potentially affect airway wall maintenance and/or remodeling, possibly relating to the genesis of bronchiectasis in autosomal dominant polycystic kidney disease, a disease of ciliopathy.

(CHEST 2009; 136:561–570)

**Abbreviations:** ADPKD = autosomal dominant polycystic kidney disease; ASM = airway smooth muscle; ECM = extracellular matrix; EGF = epidermal growth factor; EGFR = epidermal growth factor receptor; EM = electron microscopy; FAK = focal adhesion kinase; FBS = fetal bovine serum; HBSMC = human bronchial smooth muscle cell; PC = polycystin; SMA = smooth muscle  $\alpha$ -actin; VSMC = vascular smooth muscle cell

Solitary primary cilia of mammalian cells are microtubular structures protruding from cell surfaces. They arise from the basal body beneath the plasma membrane attaching to a distal centriole that locates near a proximal centriole. The distal and proximal centrioles, also termed the *diplosome*, constitute the cellular microtubule-organizing center.<sup>1,2</sup> The vast majority of primary cilia are nonmotile with a characteristic 9 + 0 axoneme organization: an annulus of nine microtubule doublets surrounding a microtubule-free center.

Research<sup>3</sup> derived from several organ systems has indicated a key role for primary cilia in mechanochemical sensing. Although a majority of cilia-related functions have been discovered in epithelial cells of tubular structures,<sup>4,5</sup> evidence for a functional role of ciliary sensing in connective tissues has been emerging. In

mouse chondrocytes and osteocytes, ciliary sensing defects created by a null mutation in *Pkd1* (a gene encodes polycystin [PC]-1, a ciliary mechanosensing protein in kidney cells) result in prominent bone deformation.<sup>3,6</sup> In mouse aortic vascular smooth muscle cells (VSMCs), primary cilia respond to mechanical deflection and integrin ligation by triggering an intracellular  $Ca^{2+}$  wave,<sup>7</sup> a recognized sign of cellular response to stimulation. Although these findings are consistent with primary cilia being a mechanochemical sensor<sup>3</sup> in connective tissues, no information exists regarding their role in airway smooth muscle (ASM) cells.

ASM cells, through their ability to sense/respond to their surrounding and to synthesize and assemble extracellular matrix (ECM),<sup>8,9</sup> are critically involved in airway development as well as airway maintenance,

remodeling, and injury repair. ASM cells interact with ECM proteins through a family of  $\alpha/\beta$  heterodimeric transmembrane integrins,<sup>10</sup> predominantly  $\alpha2$ -,  $\alpha5$ -, and  $\beta1$ -integrins.<sup>11</sup> Whether these integrins are expressed in primary cilia of ASM cells has not been previously examined.

Integrin-mediated cell-ECM interaction is complex and modulates both cytoskeleton organization and cellular signaling molecules, including Src, focal adhesion kinase (FAK), Rac GTPases, and mitogen-activated protein kinases,<sup>12,13</sup> ultimately affecting gene expression and cell proliferation, differentiation, and migration.<sup>14</sup> Moreover, research has revealed that integrins frequently partner with and activate growth factor receptor tyrosine kinases, including epidermal growth factor receptor (EGFR), hepatocyte growth factor receptor, platelet-derived growth factor receptor beta receptor, and vascular growth factor receptor. Such joint activation appears to be bidirectional<sup>14–16</sup> and has its preferred partner pairs. For instance,  $\beta1$ -integrin is shown to preferentially potentiate EGFR-mediated signaling during cell migration.<sup>16–18</sup> In this study, we examined primary cilia of human bronchial smooth muscle cells (HBSMCs), including their *in situ* distribution and orientation, mechano-chemosensory molecule expression, and function in HBSMC-ECM interaction.

## MATERIALS AND METHODS

### *Cryosections, Immunofluorescence, and Immunohistochemistry*

Intact bronchi, isolated from disease-free areas of resected lungs as surgical waste at the Mayo Clinic Rochester with the approval of the Institutional Review Board, were oriented perpendicularly or longitudinally in relation to their long axis and flash frozen/embedded as described.<sup>7</sup> The 6- $\mu$ m cryosections were immunostained with appropriate primary antibodies and preimmune serum (as negative control) and imaged with laser scanning confocal microscopy.<sup>7</sup> Immunohistochemical staining for smooth muscle  $\alpha$ -actin (SMA) was performed as previously described.<sup>19</sup>

Manuscript received November 21, 2008; revision accepted January 29, 2009.

**Affiliations:** From the Kidney Institute of the China People's Liberation Army (Drs. Wu and Mei), Changzheng Hospital, Second Military Medical University, Shanghai, People's Republic of China; and the Division of Nephrology and Hypertension (Drs. Du, Wang, and Qian), Department of Medicine, and the Department of Physiology and Biomedical Engineering (Drs. Sieck and Qian), Mayo Clinic College of Medicine, Rochester, MN.

**Funding Support:** This study was supported by National Institutes of Health grants DK63064 and DK073567, and Mayo Clinic Faculty Transition Research Award (Dr. Qian).

© 2009 American College of Chest Physicians. Reproduction of this article is prohibited without written permission from the American College of Chest Physicians ([www.chestjournal.org/site/misc/reprints.xhtml](http://www.chestjournal.org/site/misc/reprints.xhtml)).

**Correspondence to:** Qi Qian, MD, Assistant Professor of Medicine and Physiology, Division of Nephrology and Hypertension, Mayo Clinic College of Medicine, 200 First St SW, Rochester, MN 55905; e-mail: [qian.qi@mayo.edu](mailto:qian.qi@mayo.edu)  
**DOI: 10.1378/chest.08-1549**

### *Immunogold Labeling and Electron Microscopy*

The intact bronchi or primary cultured HBSMCs were processed using a standard method as detailed previously.<sup>7</sup> For transmission electron microscopy (EM), the Spurr resin-embedded samples were sectioned and imaged using an electron microscope (model 1200 electron microscope; JEOL; Tokyo, Japan). For immunogold labeling, the samples were incubated in primary antibody or normal serum at 4°C overnight, washed in phosphate-buffered saline solution, incubated with a 1.4-nm gold particle-linked secondary antibody (Nanogold; Nanoprobes; Yaphank, NY) at room temperature (for 1 h), rinsed in phosphate-buffered saline solution, and imaged using a scanning electron microscope (model 4700; Hitachi; Tokyo, Japan).

### *Primary Culture of HBSMCs and Scratch-Wound Assay*

Confluent HBSMCs (passage  $\times 2$  to  $\times 4$ ; gift from Dr. Y. S. Prakash, Mayo Clinic), which have been previously characterized,<sup>20</sup> were serum starved in 0.5% fetal bovine serum (FBS) for 96 h before experiments were conducted. For the scratch-wound assay, HBSMCs grown on cover slips were scratched linearly by a 20- $\mu$ L sterile pipette tip. After washing, several wounded areas were marked for orientation; serial phase-contrast pictures were taken at the marked areas using a microscope with a  $\times 10/0.4$  objective lens (model TE200; Nikon; Tokyo, Japan) equipped with a digital camera (Diagnostic Instruments; Sterling Heights, MI).

### *Transwell Assay*

The assay, which has been detailed elsewhere,<sup>18</sup> was performed using the following three groups of HBSMCs: (1) serum-starved (0.5% FBS for 96 h) ciliated HBSMCs; (2) nonciliated HBSMCs (non-serum starved so cilia were not developed)<sup>7,21,22</sup>; and (3) deciliated HBSMCs, ciliated cells treated with chloral hydrate (4 mmol/L for 48 h), which removes cilia by dissolving transitional fibers that anchor cilia to the plasma membrane. This method has frequently been used to study cilia-related functions.<sup>21–23</sup> The cells ( $6.0 \times 10^4$  cells per well), in triplicate, were seeded in an 8- $\mu$ m pore membrane well (Transwell; Corning; Cambridge, MA), precoated with rat-tail collagen, type 1 (1.5 mg/mL) [BD Biosciences; San Jose, CA], and incubated in 0.5% FBS Dulbecco modified Eagle medium for 12 h before fixing and Giemsa staining. The number of cells migrated through the pores were counted in 10 randomly selected  $\times 10$  microscopic fields. Parallel experiments were performed with or without epidermal growth factor (EGF) [5 ng/mL] in the lower chamber.

### *Reagents and Antibodies*

Unless specified, all reagents were obtained from Sigma-Aldrich (St. Louis, MO). Table 1 summarizes the antibodies used.

### *Statistical Analysis*

Data are expressed as the mean  $\pm$  SEM. The two-tailed Student *t* test was used for two-group comparison, and the one-way analysis of variance with Bonferroni *post hoc* analysis was used for comparing results generated from more than two groups. A *p* value of  $< 0.05$  was considered significant.

## RESULTS

### *Indirect Immunofluorescence and Electron Microscopic Localization of Primary Cilia in Human Bronchial Smooth Muscle*

Cross sections of the intact human bronchi (lumen diameter, 5 to 10 mm) were stained with hematoxylin-

**Table 1—Primary Antibodies Used in This Study**

Antigens	Species	Clone	Dilution	Source
Acetylated $\alpha$ -tubulin	Mouse	Clone 6-11B-1	1:500	Sigma Aldrich
$\gamma$ -Tubulin	Rabbit	Polyclonal	1:500	Sigma Aldrich
PC1	Rabbit	Polyclonal	1:200	Santa Cruz Biotechnology (Santa Cruz, CA)
PC1 (7e12)	Mouse	Monoclonal	1:500	See reference 16
PC2	Rabbit	Polyclonal	1:200	Santa Cruz Biotechnology
PC2 (YCC2)	Rabbit	Polyclonal	1:1,500	See reference 17
$\alpha$ 2-integrin	Rabbit	Polyclonal	1:500	Santa Cruz Biotechnology
$\alpha$ 5-integrin	Rabbit	Polyclonal	1:500	Santa Cruz Biotechnology
$\beta$ 1-integrin	Rabbit	EP1041Y	1:500	Abcam (Cambridge, MA)
EGFR	Rabbit	Polyclonal	1:500	Santa Cruz Biotechnology
SMA	Mouse	Clone 1A4	1:1,000	Sigma Aldrich

eosin (Fig 1, A and C) and SMA to confirm the HBSMC phenotype (Fig 1, A [insert]). Primary cilia in the consecutive sections were immunostained with an antibody against acetylated  $\alpha$ -tubulin, a known primary cilium marker.<sup>4</sup> As shown in Figure 1, B and D, within single ASM bundles, the cilia of individual HBSMCs distributed at roughly

the same horizontal level (within a layer approximately 2.0  $\mu$ m thick), appear as a “cilium layer.” This pattern, which was not noted in the serial longitudinal sections, was observed in all cross-sectional samples examined. No cilia were detected in parallel negative controls in which mouse IgG replaced the primary antibody.

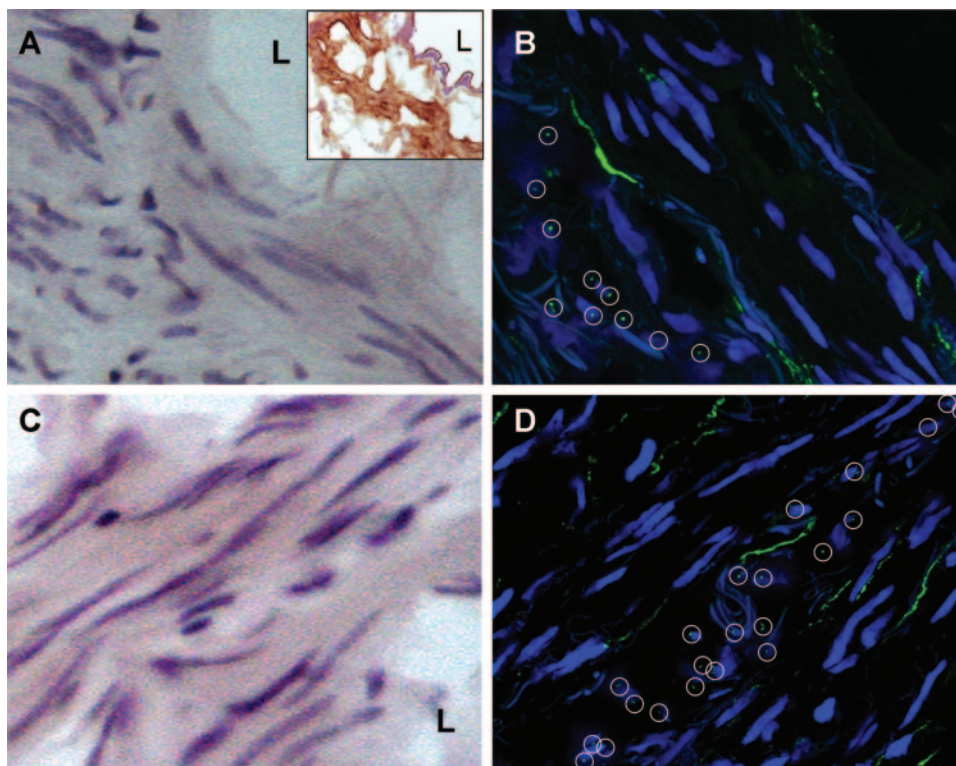


**FIGURE 1.** Primary cilia of HBSMCs are distributed as a “cilium layer” within single smooth muscle bundles. Hematoxylin-eosin staining of the cryosections from the bronchus tissue blocks show bronchial smooth muscle cells grouped in bundles that tend to have different orientations (A and C). The insert in A shows a consecutive section from the same tissue block stained for SMA in brown, confirming the HBSMC phenotype. L = lumen of the bronchus. Primary cilia (○) of HBSMCs were immunolabeled with monoclonal antibody against acetylated  $\alpha$ -tubulin, and the secondary antibody conjugated to Alexa Fluor 488 (Invitrogen; Carlsbad, CA) [B and D]. DAPI stained for the nuclei. The images were taken under a  $\times 63$  water immersion lens, showing the distribution of primary cilia in cross-sectional samples of intact bronchi.

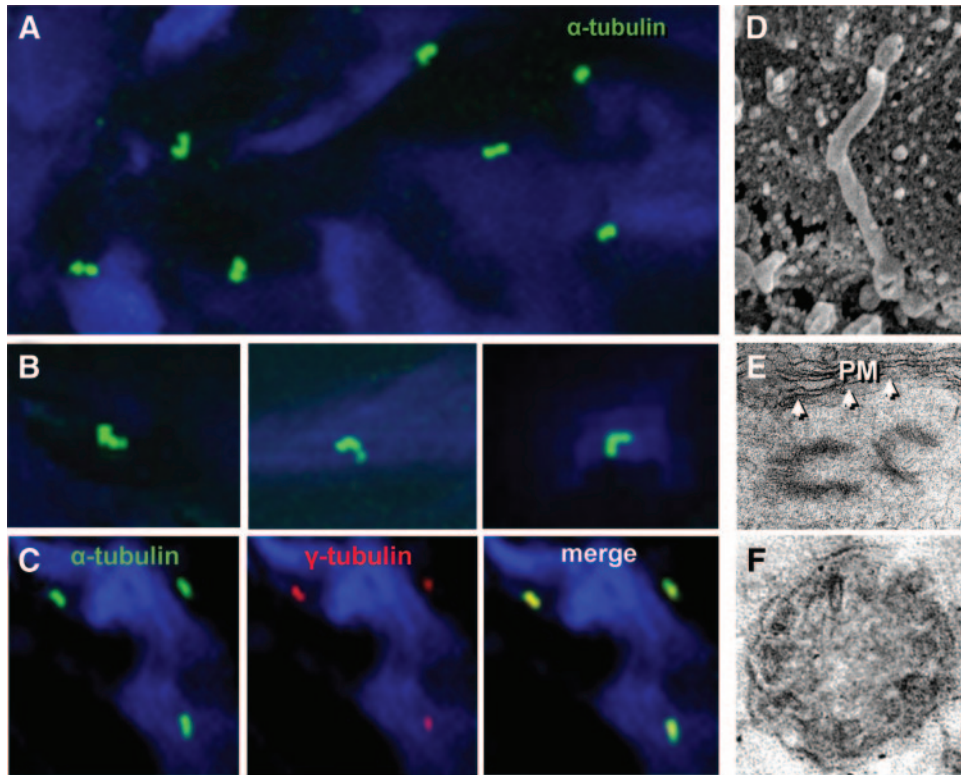


**FIGURE 2.** Primary cilia from a cilium layer, immunostained with acetylated  $\alpha$ -tubulin antibody and the secondary antibody conjugated to Alexa Fluor 488 (Invitrogen), are pointing in variable directions. **A:** DAPI stained for the nuclei. **B:** enlarged views of primary cilia from a single cilium layer, showing ciliary deflections. Primary cilia coimmunostained with acetylated  $\alpha$ -tubulin (green) for cilia and  $\gamma$ -tubulin (red) for the basal bodies. DAPI stained for the nuclei (**C**). The images in **A** and **B** were obtained with a  $\times 100$  oil immersion lens, and **C** was obtained with a  $\times 63$  water immersion lens. **D:** a scanning EM image of a primary cilium, extending out from the surface of an HBSMC. **E:** a transmission EM image of the basal diplosome adjacent to the plasma membrane (arrows) of an HBSMC. **F:** a transmission EM image of a cross section of a cilium, showing the absence of a central microtubular pair.

Under higher magnifications, primary cilia (width, approximately  $0.12\ \mu\text{m}$ ; length, approximately 2 to  $3\ \mu\text{m}$ ) were shown to protrude outward into the surrounding matrix (Fig 2, *D*). A majority exhibited varying degrees of deflection, with the distal (post-angulation) part pointing in all directions (Fig 2, *A* and *B*). Basal body and diplosome centrioles were observed by both immunolabeling of  $\gamma$ -tubulin and EM (Fig 2, *C* and *E*). EM also revealed the absence of central-pair microtubules (Fig 2, *F*) in ciliary axoneme, the ultrastructural hallmark of primary cilia.<sup>1</sup>

#### *Expression of Mechanosensing and Receptor Proteins in Primary Cilia of HBSMCs*

To determine the expression of ciliary PCs, known as mechanosensing molecules,<sup>21–23</sup> two sets of antibodies for PC1 and PC2 (Table 1) were employed. The antibodies, but not preimmune serum, clearly detected PCs in primary cilia (Fig 3, *A*).

We next examined the ciliary presence of integrins. The  $\alpha_2$ -,  $\alpha_5$ -, and  $\beta_1$ -integrins, known to be

expressed by HBSMCs,<sup>11</sup> were all localized to primary cilia (Fig 3, *B*). No signal was detected in negative controls (*B*, bottom row). Ciliary  $\beta_1$ -integrin expression was further confirmed by immunogold EM in primary cultured HBSMCs. Immunolabeled  $\beta_1$ -integrin presented as puncta in the tip and throughout shaft of cilia (Fig 3, *C*, *a* to *d*). The backscattered images<sup>24</sup> (Fig 3, *C*, *b* and *d*) allowed a better visualization of the integrin puncta. The specificity of the staining was ascertained by the absence of puncta (*e* and *f*) when the primary antibody was replaced by normal serum.

Because of the known joint activation of integrin-EGFR,<sup>18,25–27</sup> we examined ciliary EGFR expression. Figure 3, *D*, shows immunolabeled ciliary EGFR, enriched in primary cilia.

#### *Migration and Wound Filling of HBSMCs Can Be Modified by Primary Cilia*

Joint integrin-EGFR activation has been shown to modulate cell migration.<sup>14,18,25</sup> To determine

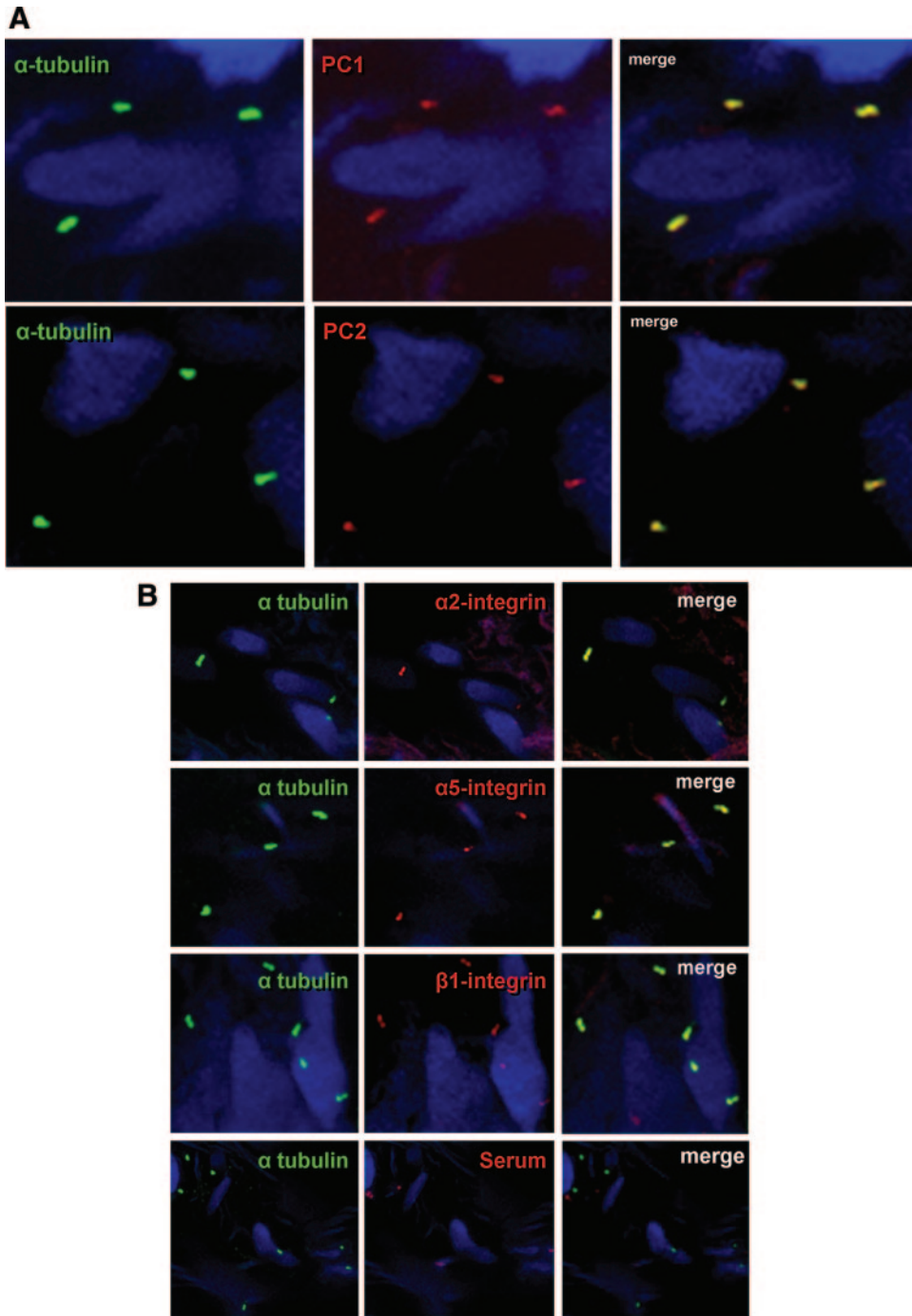


FIGURE 3. *A*: colabeling of primary cilia (green) and PC1 (red) or PC2 (red) in HBSMCs in a bronchial tissue section, showing the ciliary presence of PC1 and PC2. DAPI stained for the nuclei. *B*: colabeling of primary cilia (green) and  $\alpha$ 2-,  $\alpha$ 5-, and  $\beta$ 1-integrins (red) in HBSMCs in a bronchial tissue section. No integrin signal could be detected when the primary antibody was replaced by preimmune serum (the bottom row). DAPI stained for the nuclei. The top three panels are the images obtained with a  $\times 100$  oil immersion lens, and the bottom row was obtained with a  $\times 63$  water immersion lens. *C*: images of immunocolloidal gold scanning EM labeled for  $\beta$ 1-integrin (*a* to *d*) in primary cultured HBSMCs *b* and *d* are the corresponding backscattered images showing puncta of  $\beta$ 1-integrin; *e* and *f* are the parallel negative controls in which the primary antibody was replaced by normal serum. *D*: colabeling of cilia (green) and EGFR (red) in a bronchial tissue section showing colocalization. DAPI stained for the nuclei.

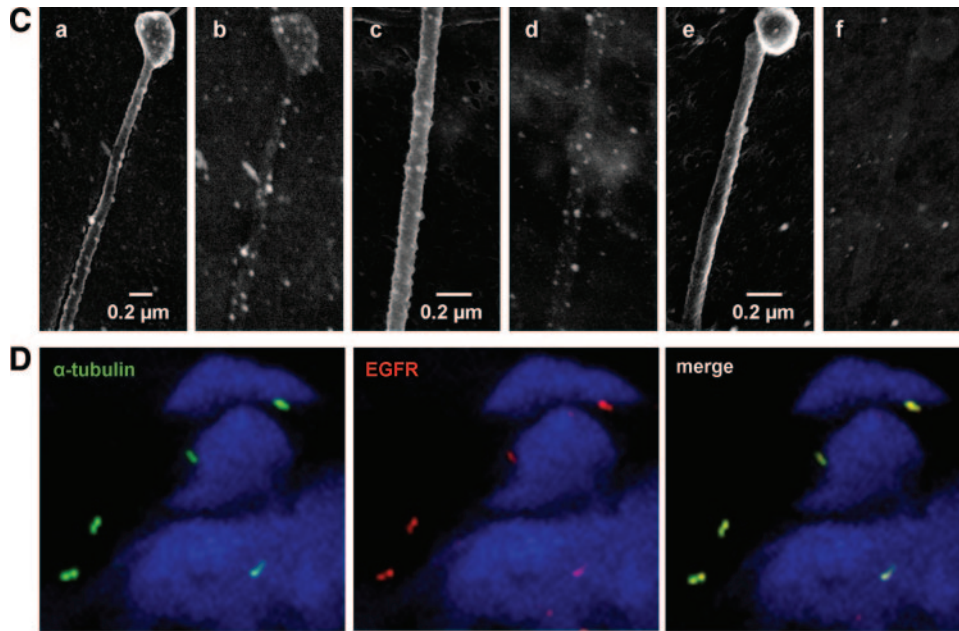


FIGURE 3. (Continued).

whether primary cilia exert a role in this process, we examined the migration pattern of HBSMCs with and without primary cilia. Ciliated, nonciliated, and deciliated HBSMCs, each in triplicate, were used; promigratory signals were created using scratch wounding and low concentration (5 ng/mL) EGF stimulation.<sup>18</sup> The cilium removal was verified (Fig 4A, right).

In the scratch-wound assay, the wounding injured the ECM and exposed matrix matricryptic sites, which are highly adhesive to integrins and are known to promote cell migration.<sup>10,28,29</sup> Thus, such wounding created a concentration gradient of high-affinity integrin ligands (matricryptic sites), with a higher ligand concentration at the injured site. EGFR is known to be coactivated under such conditions.<sup>25,26</sup> Serial phase-contrast images (at 3, 9, 12, and 24 h) revealed that the migration and wound filling were more efficient in HBSMCs with primary cilia than in those without cilia (Fig 4, A).

In an EGF-stimulated migration assay, known to involve both integrin and EGFR,<sup>18,27</sup> HBSMCs were seeded in the upper chamber (without EGF) of transwells and incubated for 12 h to allow migration to the lower chamber (with and without EGF) before fixing. The number of migrated cells in the EGF-exposed groups was  $54.1 \pm 2.03$ ,  $31.1 \pm 2.84$ , and  $33.4 \pm 1.15$ , respectively, for ciliated, nonciliated and deciliated groups ( $p < 0.001$  [one-way analysis of variance];  $n = 3$ ) [Fig 4, B]. Notably, even without EGF, ciliated cells showed a faster migration than their nonciliated and deciliated counterparts ( $17.2 \pm 1.05$ ,  $11.7 \pm 4.98$ , and  $11.5 \pm 0.06$ , respec-

tively;  $p = 0.017$ ;  $n = 3$ ). Collectively, unless ciliated, HBSMCs exhibited a decline in migration efficiency.

#### *Primary Cilia Relocate to the Interface Between HBSMCs and the Wound*

We further examined the distribution of primary cilia during HBSMC migration in the scratch-wound assay. Notwithstanding the faint background autofluorescence, the labeling of primary cilia was robust and easily recognizable. Although no specific distribution pattern could be found in noninjured areas (Fig 5, A), a majority of cilia at the wound edge were aligned between the nuclei and wound space (Fig 5, B to D). At 9 h after the wounding,  $78.8 \pm 2.5\%$  of cilia ( $n = 3$ ) were positioned ahead of the nuclei facing the wound. This finding is reminiscent of previous observations in other cell systems<sup>7,30,31</sup> and infers a role for cilia in directing cell migration.

To determine whether integrins contribute to such cilia relocation, we repeated the same study in HBSMCs pretreated with  $\beta 1$ -integrin blocker (BD Biosciences), 16  $\mu\text{g}/\text{mL}$ . The percentage of cilia relocation was reduced (Fig 5, E) from  $78.8 \pm 2.5\%$  to  $57.4 \pm 8.3\%$  ( $p = 0.039$ ;  $n = 3$ ), suggesting a contribution of the ciliary integrin-matrix interaction, at least in part, in the cilia relocation.

## DISCUSSION

In this study, we show that the primary cilia of ASM cells in human bronchi exhibit a patterned

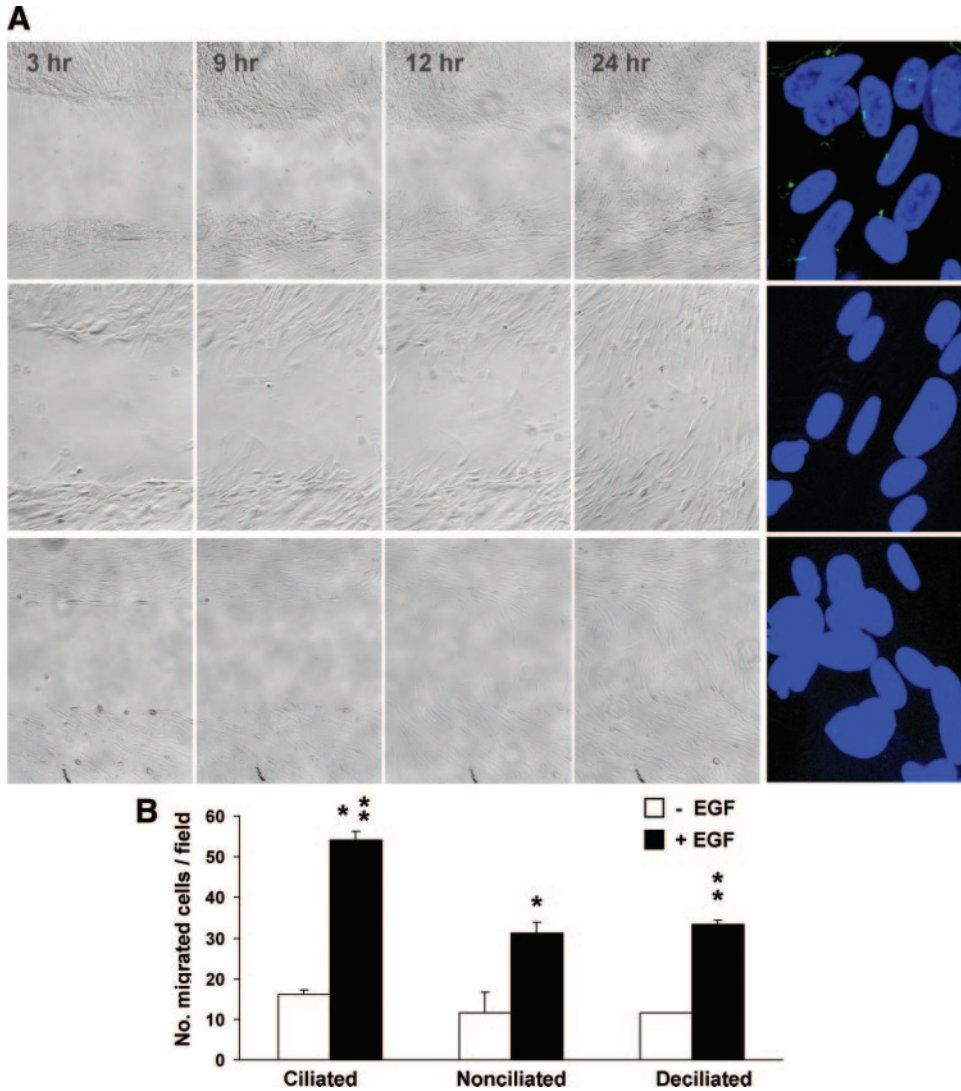


FIGURE 4. *A*: scratch-wound assay of ciliated (*left panel, top row*), nonciliated (*center row*), and deciliated (*bottom row*) HBSMCs, showing that both the nonciliated and deciliated cells migrate less efficiently with a delay in wound healing. Immunostaining of primary cilia in the ciliated, nonciliated, and deciliated HBSMCs with antiacetylated  $\alpha$ -tubulin and the secondary antibody conjugated to Alexa Fluor 488 (Invitrogen) [*far right panel*]. DAPI stained for the nuclei. Twenty-five consecutive confocal images were stacked to confirm the presence or the absence of cilia. *B*: transwell migration assay of ciliated, nonciliated, and deciliated HBSMCs. The bars represent the number of cells that migrated after 12 h with (black bars) or without (clear bars) 0.5 ng/mL EGF stimulation. The numbers of migrated cells in EGF stimulated groups were  $54.1 \pm 2.03$ ,  $31.1 \pm 2.84$ , and  $33.4 \pm 1.15$ , respectively, in ciliated, nonciliated, and deciliated groups ( $p < 0.001$  [ciliated vs nonciliated and deciliated groups;  $n = 3$ ]).

distribution, contain essential membrane receptors and channel proteins, and influence cell migration and wound healing, with a role for integrin–EGFR-mediated signaling.

ASM cells and their surrounding ECM interact intimately. ASM cells control the abundance and topology of ECM; mechanochemical signals from the ECM influence the contractile properties<sup>32</sup> and phenotype<sup>33,34</sup> of ASM cells. Such interactions are critical for meeting the varying environmental de-

mands, including mechanical stretching and injury, to which the airway is subject. However, to date there is no clear understanding of how these interactions take place. We show that primary cilia of HBSMCs extend up to approximately 2  $\mu\text{m}$  into ECM. Such positioning, combined with their inherent features, that is, large surface/volume ratio and minute size (approximately 4,000-fold smaller than a cell<sup>5</sup>), is ideal for high-sensitivity sensing and interfacing. Moreover, within single ASM bundles, cilia

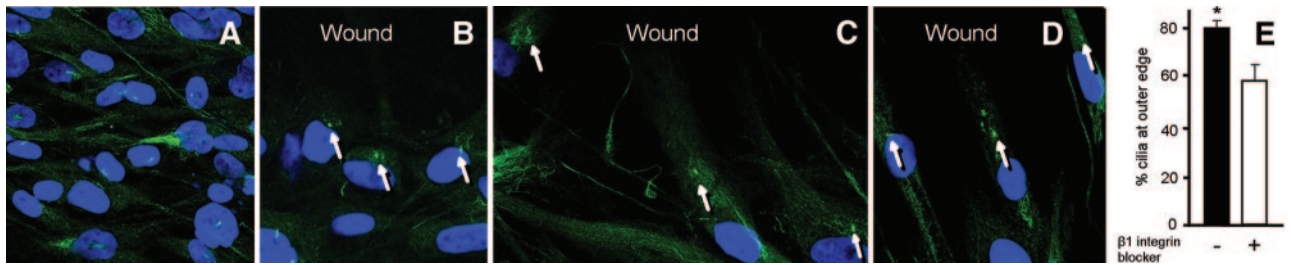


FIGURE 5. A: primary cultured HBSMCs before scratch wounding, showing that primary cilia (green), immunostained with antibody to acetylated  $\alpha$ -tubulin, are distributed randomly. B to D: after scratch wounding for 6, 9, and 12 h, primary cilia (green) were positioned in the direction of the wounding and ahead of the nuclei (arrows indicate primary cilia). DAPI stained for the nuclei. E: when HBSMCs were treated with  $\beta$ 1-integrin blocker (16  $\mu$ g/mL), the mean percentage of cilia relocated to the wound edge was reduced from  $78.8 \pm 2.5\%$  without  $\beta$ 1-integrin blocker to  $57.4 \pm 8.3\%$  with  $\beta$ 1-integrin blocker ( $p = 0.039$ ,  $n = 3$ ).

assume a horizontally layered distribution (in cross sections of the bronchi) [Fig 1, B and D]. Whether such patterned distribution, different from that in VSMCs,<sup>7</sup> pertains to functional significance is unknown. However, if a given ASM bundle functions as a unit, one might speculate that a layered distribution would facilitate a regional signal sensing as well as signal relay among the cilia in close proximity, favoring a synchronized regional response to stimulation.

High-magnification images revealed that the vast majority of cilia exhibited varying degrees of deflection (Fig 2), a marker of mechanical forces imposed onto the cilia.<sup>5</sup> Cilia have been shown, in kidney cells<sup>23,35</sup> and VSMCs,<sup>7</sup> to sense and relay such mechanical signals to the cell interior through a PC-mediated  $Ca^{2+}$  response. Although confirmatory study is necessary, *in situ* ciliary deflection and an enriched ciliary PC expression (Fig 3, A) suggest that primary cilia possibly mediate mechanosensing in ASM.

The migration of ASM cells, which is important for airway development and remodeling,<sup>8</sup> is influenced by a joint activation of integrins and receptor tyrosine kinases, through their downstream FAK and Src signaling.<sup>18,36</sup> The demonstration of the ciliary enrichment of the major FAK and Src activators, integrins, and EGFR (Fig 3, B to D), supports a possible scenario whereby primary cilia, through ciliary integrin-EGFR signaling, affect ASM cell migration.

This possibility was examined directly. Two experimental methods, designed to enhance integrin or EGFR ligation, produced similar results. Ciliated HBSMCs migrate and fill the wound much more efficiently than their nonciliated and deciliated counterparts (Fig 4), which is consistent with a ciliary contribution in this process, possibly through integrin and/or EGFR-mediated signaling. It should be noted, however, that even without cilia, HBSMCs still migrate (albeit much less efficiently), indicating

that primary cilia may not be a dominant determinant in the migratory process. Multiple overlapping pathways, several of which have been well characterized,<sup>8</sup> likely converge to accomplish this task. Our results, nevertheless, strongly suggest a modulatory role of primary cilia in ASM cell migration.

We further observed a tight association between an optimal HBSMC migration/wound filling and a repositioning of cilia to the wound edge, giving an appearance of “cilia leading the way” (Fig 5). Similar ciliary alignment was described in migrating rat 3Y1 cells<sup>30,31,37</sup> and 3T3 fibroblasts.<sup>37</sup> The present study extends the previous findings by demonstrating an enriched ciliary expression of integrins and EGFR, an integrin-dependent ciliary repositioning, and ciliary contribution to an efficient wound filling. The linkage of cilia and ciliary integrins/EGFR to migration and wound healing in ASM cells is novel.

The importance of ciliary mechanochemical sensing has been demonstrated in several human diseases. The most extensively studied ciliopathy in recent years is autosomal dominant polycystic kidney disease (ADPKD), a common genetic disease caused by mutations in *PKD1* or *PKD2* gene (encoding PC1 or PC2), and characterized by polycystic kidney enlargement and kidney failure.<sup>22,35</sup> Patients with ADPKD also exhibit prominent connective tissue abnormalities,<sup>38</sup> including abnormal arterial remodeling, intracranial aneurysms, hernia/diverticula, and dilation of the pericardium with pericardial effusion.<sup>39</sup> Recent studies<sup>40,41</sup> also show an approximately threefold increase in the occurrence of bronchiectasis in patients with ADPKD. Moreover, the bronchiectasis is frequently coupled with irregular bronchial wall thickness, without evidence of recurrent airway infection, inferring airway wall defects and possible ASM involvement.

How the ciliopathy in ADPKD might link to the bronchiectasis warrants further investigation. We speculate that primary cilia of ASM cells likely function as mechanical/pressure sensors; *PKD* gene



mutations might alter ASM pressure sensing. Additionally, studies have suggested that PCs complex with integrins and EGFR<sup>42–44</sup>; *PKD* gene mutations, therefore, might interfere with the functions of these molecules because a migration defect was observed in *Pkd1* mutant kidney cells.<sup>45</sup>

In summary, we show that primary cilia of ASM cells are strategically distributed, favoring a synchronized response to stimulation; they express a number of molecules critical for mechanochemical sensing, and modulate cell migration and injury repair. These findings, combined with the increased occurrence of bronchiectasis in ADPKD, suggest a role for primary cilia in airway maintenance and remodeling.

#### ACKNOWLEDGMENTS

**Author contributions:** Dr. Qian designed the experiments, analyzed the data, and wrote the paper. Drs. Wu, Du, and Wang conducted experiments and contributed to the data analysis. Drs. Mei and Sieck contributed to the designing of the experiments. **Financial/nonfinancial disclosure:** The authors have reported to the ACCP that no significant conflicts of interest exist with any companies/organizations whose products or services may be discussed in this article.

#### REFERENCES

- Satir P, Christensen ST. Overview of structure and function of mammalian cilia. *Annu Rev Physiol* 2007; 69:377–400
- Kellogg DR, Field CM, Alberts BM. Identification of microtubule-associated proteins in the centrosome, spindle, and kinetochore of the early *Drosophila* embryo. *J Cell Biol* 1989; 109:2977–2991
- Singla V, Reiter JF. The primary cilium as the cell's antenna: signaling at a sensory organelle. *Science* 2006; 313:629–633
- Poole CA, Jensen CG, Snyder JA, et al. Confocal analysis of primary cilia structure and colocalization with the Golgi apparatus in chondrocytes and aortic smooth muscle cells. *Cell Biol Int* 1997; 21:483–494
- Poole CA, Flint MH, Beaumont BW. Analysis of the morphology and function of primary cilia in connective tissues: a cellular cybernetic probe? *Cell Motil* 1985; 5:175–193
- Xiao Z, Zhang S, Mahlios J, et al. Cilia-like structures and polycystin-1 in osteoblasts/osteocytes and associated abnormalities in skeletogenesis and Runx2 expression. *J Biol Chem* 2006; 281:30884–30895
- Lu C, Du H, Wu J, et al. Non-random distribution and sensory functions of primary cilia in vascular smooth muscle cells. *Kidney Blood Press Res* 2008; 31:171–184
- Gerthoffer WT. Migration of airway smooth muscle cells. *Proc Am Thorac Soc* 2008; 5:97–105
- Halayko AJ, Solway J. Molecular mechanisms of phenotypic plasticity in smooth muscle cells. *J Appl Physiol* 2001; 90:358–368
- Hynes RO. Integrins: bidirectional, allosteric signaling machines. *Cell* 2002; 110:673–687
- Nguyen TT, Ward JP, Hirst SJ. Beta1-integrins mediate enhancement of airway smooth muscle proliferation by collagen and fibronectin. *Am J Respir Crit Care Med* 2005; 171:217–223
- Juliano RL, Reddig P, Alahari S, et al. Integrin regulation of cell signalling and motility. *Biochem Soc Trans* 2004; 32:443–446
- Marcoux N, Vuori K. EGF receptor mediates adhesion-dependent activation of the Rac GTPase: a role for phosphatidylinositol 3-kinase and Vav2. *Oncogene* 2003; 22:6100–6106
- Giancotti FG, Tarone G. Positional control of cell fate through joint integrin/receptor protein kinase signaling. *Annu Rev Cell Dev Biol* 2003; 19:173–206
- Berk BC. Vascular smooth muscle growth: autocrine growth mechanisms. *Physiol Rev* 2001; 81:999–1030
- Moro L, Venturino M, Bozzo C, et al. Integrins induce activation of EGF receptor: role in MAP kinase induction and adhesion-dependent cell survival. *EMBO J* 1998; 17:6622–6632
- Miyamoto S, Teramoto H, Gutkind JS, et al. Integrins can collaborate with growth factors for phosphorylation of receptor tyrosine kinases and MAP kinase activation: roles of integrin aggregation and occupancy of receptors. *J Cell Biol* 1996; 135:1633–1642
- Sieg DJ, Hauck CR, Ilic D, et al. FAK integrates growth-factor and integrin signals to promote cell migration. *Nat Cell Biol* 2000; 2:249–256
- Qian Q, Hunter LW, Du H, et al. *Pkd2*+/- vascular smooth muscles develop exaggerated vasoconstriction in response to phenylephrine stimulation. *J Am Soc Nephrol* 2007; 18:485–493
- Prakash YS, Thompson MA, Vaa B, et al. Caveolins and intracellular calcium regulation in human airway smooth muscle. *Am J Physiol Lung Cell Mol Physiol* 2007; 293: L1118–L1126
- Praetorius HA, Spring KR. Removal of the MDCK cell primary cilium abolishes flow sensing. *J Membr Biol* 2003; 191:69–76
- Praetorius HA, Spring KR. Bending the MDCK cell primary cilium increases intracellular calcium. *J Membr Biol* 2001; 184:71–79
- Praetorius HA, Frokiaer J, Nielsen S, et al. Bending the primary cilium opens Ca<sup>2+</sup>-sensitive intermediate-conductance K<sup>+</sup> channels in MDCK cells. *J Membr Biol* 2003; 191:193–200
- Suzuki K, Nakajima C, Moriyama M, et al. Backscattered electron imaging of crystal matrix protein on the surface of calcium oxalate crystals using colloidal gold. *Int J Urol* 1995; 2:87–91
- Mariotti A, Kedeshian PA, Dans M, et al. EGF-R signaling through Fyn kinase disrupts the function of integrin alpha6beta4 at hemidesmosomes: role in epithelial cell migration and carcinoma invasion. *J Cell Biol* 2001; 155:447–458
- Moro L, Dolce L, Cabodi S, et al. Integrin-induced epidermal growth factor (EGF) receptor activation requires c-Src and p130Cas and leads to phosphorylation of specific EGF receptor tyrosines. *J Biol Chem* 2002; 277:9405–9414
- Cabodi S, Moro L, Bergatto E, et al. Integrin regulation of epidermal growth factor (EGF) receptor and of EGF-dependent responses. *Biochem Soc Trans* 2004; 32:438–442
- Martinez-Lemus LA, Wu X, Wilson E, et al. Integrins as unique receptors for vascular control. *J Vasc Res* 2003; 40:211–233
- Faull RJ, Kovach NL, Harlan JM, et al. Affinity modulation of integrin alpha 5 beta 1: regulation of the functional response by soluble fibronectin. *J Cell Biol* 1993; 121:155–162
- Albrecht-Buehler G. Phagokinetic tracks of 3T3 cells: parallels between the orientation of track segments and of cellular structures which contain actin or tubulin. *Cell* 1977; 12:333–339
- Katsumoto T, Higaki K, Ohno K, et al. The orientation of primary cilia during the wound response in 3Y1 cells. *Biol Cell* 1994; 81:17–21
- Bramley AM, Roberts CR, Schellenberg RR. Collagenase increases shortening of human bronchial smooth muscle *in vitro*. *Am J Respir Crit Care Med* 1995; 152:1513–1517
- Hirst SJ, Twort CH, Lee TH. Differential effects of extracellular matrix proteins on human airway smooth muscle cell

- proliferation and phenotype. *Am J Respir Cell Mol Biol* 2000; 23:335–344
- 34 Parameswaran K, Radford K, Zuo J, et al. Extracellular matrix regulates human airway smooth muscle cell migration. *Eur Respir J* 2004; 24:545–551
- 35 Nauli SM, Alenghat FJ, Luo Y, et al. Polycystins 1 and 2 mediate mechanosensation in the primary cilium of kidney cells. *Nat Genet* 2003; 33:129–137
- 36 Kaplan KB, Swedlow JR, Morgan DO, et al. c-Src enhances the spreading of src<sup>-/-</sup> fibroblasts on fibronectin by a kinase-independent mechanism. *Genes Dev* 1995; 9:1505–1517
- 37 Albrecht-Buehler G, Bushnell A. The orientation of centrioles in migrating 3T3 cells. *Exp Cell Res* 1979; 120:111–118
- 38 Grantham JJ. Clinical practice: autosomal dominant polycystic kidney disease. *N Engl J Med* 2008; 359:1477–1485
- 39 Qian Q, Hartman RP, King BF, et al. Increased occurrence of pericardial effusion in patients with autosomal dominant polycystic kidney disease. *Clin J Am Soc Nephrol* 2007; 2:1223–1227
- 40 Driscoll JA, Bhalla S, Liapis H, et al. Autosomal dominant polycystic kidney disease is associated with an increased prevalence of radiographic bronchiectasis. *Chest* 2008; 133:1181–1188
- 41 Wu J, Du H, Jensen D, et al. Increased incidence of bronchiectasis in ADPKD and the role of primary cilia in human airway smooth muscle cells. *J Am Soc Nephrol* 2008; 19:125A
- 42 Malhas AN, Abuknesha RA, Price RG. Interaction of the leucine-rich repeats of polycystin-1 with extracellular matrix proteins: possible role in cell proliferation. *J Am Soc Nephrol* 2002; 13:19–26
- 43 Wilson PD, Geng L, Li X, et al. The PKD1 gene product, “polycystin-1,” is a tyrosine-phosphorylated protein that colocalizes with  $\alpha\beta$ 1-integrin in focal clusters in adherent renal epithelia. *Lab Invest* 1999; 79:1311–1323
- 44 Ma R, Li WP, Rundle D, et al. PKD2 functions as an epidermal growth factor-activated plasma membrane channel. *Mol Cell Biol* 2005; 25:8285–8298
- 45 Boca M, D’Amato L, Distefano G, et al. Polycystin-1 induces cell migration by regulating phosphatidylinositol 3-kinase-dependent cytoskeletal rearrangements and GSK3 $\beta$ -dependent cell cell mechanical adhesion. *Mol Biol Cell* 2007; 18:4050–4061